Long-term persistence of crAss-like phage crAss001 is associated with phase variation in *Bacteroides intestinalis*

Andrey N. Shkoporov*[1], Ekaterina V. Khokhlova*[1], Niamh Stephens[2], Cara Hueston[1], Samuel Seymour[1], Dimitri Scholz[2], R. Paul Ross[1], Colin Hill[1]

*These authors contributed equally to the study.
1. APC Microbiome Ireland and School of Microbiology, University College Cork, Cork, Ireland
2. Conway Institute of Biomolecular and Biomedical Research, University College Dublin, Belfield, Dublin 4, Ireland

Abstract

The crAss-like phages are ubiquitous and highly abundant members of the human gut virome that infect commensal bacteria of the order Bacteroidales. Although incapable of classical lysogeny, these viruses demonstrate unexplained long-term persistence in the human gut microbiome, dominating the virome in some individuals. Here we demonstrate that rapid phase variation of alternate capsular polysaccharides plays an important role in dynamic equilibrium between phage sensitivity and resistance in *B. intestinalis* cultures, allowing phage and bacteria to multiply in parallel. The data also suggests the role of concomitant phage persistence mechanisms associated with delayed lysis of infected cells, such as carrier state infection. From an ecological and evolutionary standpoint this type of phage-host interaction is consistent with the Piggyback-the-Winner model, which suggests a preference towards lysogenic or other “benign” forms of phage infection when the host is stably present at high abundance.

Keywords: crAss-like phages; human gut microbiome; human virome; phase variation; capsular polysaccharides; carrier state infection.

Introduction

The crAss-like bacteriophages are a recently described family of dsDNA tailed bacterial viruses of the order Caudovirales that are predicted to infect bacteria of the phylum Bacteroidetes (Yutin et al., 2020). They are present in variety of host-associated, aquatic and terrestrial habitats, but are especially predominant in the human gut (Honap et al., 2020; Koonin and Yutin, 2020; Yutin et al., 2018). The presence of the prototypical crAssphage (p-crAssphage) in >70% of human gut metagenomes together with its exceptional abundance in some of the samples (>90% of the gut virome and >20% of total faecal DNA) led to its description as “the most abundant virus of the human body” (Yutin et al., 2018). Furthermore, p-crAssphage was found to be widespread in the global human population with sequence variants correlating with geographic location (Edwards et al., 2019). Based on the observation of related genomes in the non-human primate gut, it was proposed that p-crAssphage shares a long co-evolutionary history with the human species. In addition, limited dietary associations, but no link to disease was observed in crAssphage colonisation patterns (Koonin and Yutin, 2020).

A recent longitudinal study of the human gut virome highlighted long-term (months and even years) high-level persistence of different combinations of crAss-like phages across individuals (Shkoporov et al., 2019). When vertically transmitted from mothers to their infants or transplanted into in the

course of faecal microbial transplantation (FMT), crAss-like phage engraft successfully and stably persist for many months (Draper et al., 2018; Siranosian et al., 2020). CrAss-like phages can also persist in pure bacterial culture *in vitro* over many serial passages without any significant effect on the density of host population (Shkoporov et al., 2018). The overall effect of stably persisting crAss-like phages, sometimes reaching absolute concentrations of 10^{11} genome copies per gram (Shkoporov et al., 2019), on the structure (composition) and function of the gut microbiome is yet to be determined. Despite a lack of disease associations with p-crAssphage, correlations with other candidate genera and individual strains within the family of crAss-like phages has not been examined. Certain recent studies hinted at depletion of certain crAss-like viral clusters in an IBD patient cohort (Clooney et al., 2019), while at the same time a genus VI crAss-like phage, termed IAS virus, was prevalent in HIV patients with unexplained diarrhoea (Oude Munnink et al., 2014). It remains unclear what mechanisms are responsible for the long-term persistence and high prevalence of crAss-like phages in the human gut. Several mechanisms of phage persistence are possible, including spatial heterogeneity of microbial habitats in the gut (Lourenço et al., 2020), physiological stochasticity of phage sensitivity phenotype in their host bacteria (Lourenço et al., 2018), reversible genetic switching (phase variation) of surface receptor expression (Porter et al., 2020), constant sweeps of new mutations leading to arms race co-evolution with their hosts (Scanlan, 2017), or perhaps, an unusual life cycle (carrier state infection, pseudolysogeny) of the viruses themselves.

Establishing these mechanism(s) is a challenging task due to the lack of tools for genetic manipulation, and the low similarity of crAss-like phage genomes and proteins to well characterised model viruses (Dutilh et al., 2014). Our limited understanding of certain biological properties of crAss-like phages derives from ΦcrAss001 (candidate genus VI), the first cultured member of the crass-like phages (Shkoporov et al., 2018).

Here, we report the first comprehensive effort to characterise interaction of ΦcrAss001 with its host and certain mechanisms involved in its long term persistence. We demonstrate that phase variation of capsular polysaccharides creates dynamic sub-populations of sensitive and resistant *Bacteroides* cells, leading to long term persistence. A yet unexplained mechanism is apparently responsible for a paused infection cycle and delayed release of phage progeny from a significant fraction of infected cells, a phenomenon that may represent a novel type of carrier state infection.

Results

CrAss-like phages are capable of long-term stable persistence in the mammalian gut and select for resistance in their bacterial host

We have previously demonstrated the long-term persistence of crAss-like phages in the human gut microbiome (Shkoporov et al., 2019). The levels of crAss-like phage colonisation in ten subjects varied from <10% of the total faecal virome to nearly 100%. Eight of the ten subjects were stably colonised by one or several individual crAss-like phage strains.

Different crAss-like phage genera tended to colonise with distinctive relative abundances. High level colonisation with relative abundances approaching 100% of the virome were typical of genus I, whereas genus VI had much lower relative abundance, possibly reflecting differences in their host abundance, mode of replication, or the rate of emergence of resistance in the host strains (**Fig. 1a**). To reinforce this observation we followed the dynamics of crAss-like phage persistence in a monoxenic mouse model using the first cultivable representative of the family, ΦcrAss001. Mice (n

= 6) colonised with *B. intestinalis* alone served as a negative control. Within the first few days upon bacterial gavage, faecal *B. intestinalis* reached levels of 10^{11} cfu g^{-1} regardless of the presence of phage ($p>0.05$ in Kruskal-Wallis test with FDR correction for all time points except day 31). ΦcrAss001 propagated to much lower levels of 10^6-10^8 pfu g^{-1}. However, this level also remained until the termination of the experiment at 136 days (**Fig. 1b**).

Long term persistence of the phage-host pair quickly induces resistance to ΦcrAss001 in *B. intestinalis*. By day three from the first gavage, 11/17 (65%) of *B. intestinalis* faecal isolates were completely resistant to phage in spot and plaque assays, compared to 2% of spontaneously resistant cells in an overnight broth culture grown in the absence of phage (see below). By week twelve, 15/29 (52%) isolates were resistant. The sensitive isolates showed varied degrees of partial resistance that was manifested by formation of spots of variable turbidity. Unexpectedly, even bacterial isolates from the control animals showed a switch towards the phage-resistant phenotype in that while day three isolates were all sensitive (17/17), 8/29 (27%) isolates from week twelve were completely resistant, showing that a switch between sensitive and resistant phenotypes can occur in the host strain independently of phage attack.

This persistence can be recapitulated *in vitro*, in a *B. intestinalis* culture infected in its early logarithmic phase at multiplicity of infection (MOI) of 1, followed by overnight incubation and daily passages of resulting phage-bacterial co-culture. Initial absorption of phage resulted in 96.5% reduction of bacterial CFU after 30 min (**Fig. 1c**), followed by the first round of phage genome replication, which was largely completed by 90 min after infection resulting in a calculated virus-to-microbe ratio (VMR) of ~22.8±1.2 (median±IQR, **Fig. 1d**). Parallel propagation of bacteria and phage for the first 24 hours maintained roughly the same level of VMR and resulted in high titre of phage particles $3.86 \times 10^{10} \pm 7 \times 10^9$ pfu ml^{-1} (**Fig. 1bc)**. Subsequent daily transfers led to a drop of VMR and phage titres, but resulted in increased viable bacterial titres and a phage/host dynamic that is stably maintained for as many as 23 daily transfers (**Fig. 1d**). This evidence again points towards a rapid shift to dominance by resistant cells while retaining a sufficient sensitive sub-population to allow for low level reproduction and persistence.

Resistance of B. intestinalis cells to ΦcrAss001 develops at high rate in vitro, but is reversible and associated with inhibition of phage adsorption

ΦcrAss001 forms turbid spots in soft agar overlays containing *B. intestinalis* APC919/174, confirming that bacterial growth can occur in the presence of phage (**Fig. 2a**). This could be a result of a high rate of lysogeny, or of a pre-existing resistant sub-population. Spontaneous point mutations are less likely to explain this phenomenon as their typically much lower frequencies would result in the formation of isolated colonies rather than diffuse growth. Transmission electron microscopic (TEM) examination was conducted on the centre of each spot. Contrary to our expectations, the electron micrographs of spot material revealed the presence of both uninfected and infected cells among the cell debris, including many instances in which cells in the process of division had phage progeny restricted to only one of the two nascent daughter cells (**Fig. 2b-f**). This suggests that the resistance phenotype may in fact be unstable, and that periodic switching to a sensitive phenotype occurs in surviving cells, leading to secondary waves of infections.

In the presence of an excess of phage in soft agar overlays (efficiency of plating assay, EOP), clonal cultures of *B. intestinalis* APC919/174 had 2.06±0.14% (mean±SD) immediate resistance rate (**Fig. 2g-h**, which agrees with 96.5% cells being infected above). None of the tested colonies contained

DNA of ΦcrAss001 detectable by PCR. Ten resistant clones were each sub-cultured 12 separate times, four of the 120 (3.3%) reverted to sensitive phenotype. Resistant clones demonstrated a dramatically reduced ability to adsorb phage, while the spontaneously sensitive 'revertants' had restored phage adsorption (**Fig. 2j**). Some of the sub-clones had altered colony morphologies, with resistant colonies being more transparent, while sensitive ones were opaque (e.g. sub-clones 8T and 8W in **Fig. 2i**). When a resistant clone 8T was subjected to an EOP assay the rate of survival was raised to 88.7±3.3%, but in the sensitive sub-clone 8W it had returned closer to the original level of 11.3±0.9%. TEM of 8T cells revealed an altered "hairy" appearance, with a loose and bulky polymeric substance indicative of production of a different type of capsular polysaccharide (CPS) (**Fig. 2k**). In contrast, the wild-type (WT) culture demonstrates a much more compact thinner layer of capsular polysaccharide intimately attached to the outer membrane (**Fig. 2l**).

Together, this data suggests that cultures of *B. intestinalis* contain mixed populations of cells, where an equilibrium between different states of cell surface and phage-sensitivity status results from constant reversible switching through some genetic or epigenetic mechanism. Approximately 2% of cells in naïve cultures were resistant to phage. Exposure to phage in continuous culture *in vitro* or in the murine gut drives the bacterial population towards phage resistance, but this never reaches 100% or leads to the extinction of the phage.

Phase variation of multiple surface loci and concomitant capsular polysaccharide switching in B. intestinalis

In order to identify the mechanism of resistance we subjected ten resistant clones and two revertant sensitive sub-clones to whole genome sequencing. We also performed sequencing of samples collected from the long-term *in vitro* persistence experiment 5 min – 28 days following the inoculation and some of the faecal samples collected in long term murine colonisation experiment. For the wild type strain, resistant clone 8T ("transparent") and its corresponding revertant clone 8W ("white"), complete circular genomes were assembled. A comparison of the three assemblies revealed that the only detectable differences consist of the inversion and rearrangement of several genomic loci (**Fig. S1a**). Three types of events were detectable, including, (a), large inversions involving entire gene clusters comprised of genes coding for TonB-dependent transporters (Bolam and van den Berg, 2018) and/or RagB/SusD-like nutrient uptake proteins (Foley et al., 2016), often flanked with a dedicated integrase/recombinase gene; (b), a more complex type of reshuffling of clusters containing ABC-transporter genes (**Fig. S1b**); and (c), the inversion of small, <200 bp regions adjacent to capsular polysaccharide biosynthesis operons that contain potential promoters. Remarkably, all these genomic loci, designated as "phase variable regions" (PVRs), can be directly implicated in phage sensitivity. Their encoded products are either components of cell surface structures with potential to serve as receptors or barriers for phage adsorption or potential phage defence molecules (e.g. restriction/modification system).

Transcriptomic analysis of serial daily broth co-cultures of *B. intestinalis* and ΦcrAss001 1-5 days after the initial inoculation revealed an array of genes showing divergent responses to the presence of phage ($p<0.001$, DESeq2). The strongest transcriptional response in the host cells, already visible after the first 24 h, was associated with PVRs and consisted in the strong ~100-fold repression of the PVR9 capsular polysaccharide (CPS) biosynthesis operon, the up-regulation of similar CPS operons associated with loci PVR7, PVR8 and PVR11 (**Fig. 3a**), and the up-regulation of a group of nutrient uptake genes in a complete inversion of the integrase/recombinase gene-flanked operon

PVR3. Importantly, similar alterations of gene expression patterns relative to the phage-naïve WT culture of *B. intestinalis* can be observed in the resistant clone 8T (in the absence of phage). Its phage sensitive derivative 8W displays restored levels of PVR9 expression, down-regulated (compared to WT) PVR7, PVR8 and PVR11 and up-regulated expression of PVR3.

The CPS-encoding loci PVR7-11 have broadly differing gene content with limited levels of amino acid homology between certain shared protein orthologues (e.g. oligosaccharide flippases, dehydrogenases, dehydratases and glycosyl transferases; **Fig. 3b**). All of these loci share a putative invertible, moderately conserved promoter sequence of 183-186 bp (**Fig. 3c**) flanked by a perfect, completely conserved 10 bp inverted repeat GTTCGTTTAA at which recombination most likely occurs. This sequence partially overlaps with inverted repeats ARACGTTCGTN flanking phase variable promoters controlled by a serine recombinase family, master DNA invertase (mpi) in *Bacteroides fragilis* (Coyne et al., 2003). At least two homologs of this enzyme are encoded in the genome of *B. intestinalis* APC919/174 (NCBI accession QDO70032.1 and QDO69715.1). A search for similar patterns in the *B. intestinalis* APC919/174 genome revealed the presence of an additional, fifth, CPS locus (denoted PVR12) with identical inverted repeat flanking its promoter region. This locus, however, did not show significant up- or down-regulation of expression in our RNAseq assays. By mapping the RNAseq reads we located the approximate transcription start in PVR7-11 inside the proximal copy of the inverted repeat (**Fig. 3c**), confirming that the invertible regions are capable of acting as promoters.

To explore the rate and frequency of phase variation on the complete genome scale and to identify other potential PVRs, we performed local alignment of individual long DNA reads (obtained from WT culture, resistant clones 8T and PhR5, and corresponding revertant sub-clones 8W and PhR5-1) to the assembled circular genome reference, searching for cases where parts of the same long read align inconsistently, indicating either inversion or translocation. This analysis revealed a series of strong recombination hotspots present in every culture tested. The majority were associated with already known PVRs, with exception of a few novel finds, one of which is the previously mentioned fifth CPS locus PVR12 (**Fig. S2**). We then used mapping of short shotgun reads to allow the quantitation of inversions in the long term *in vitro* and *in vivo* persistence experiments, ten resistant clones and one revertant sub-clone. By aligning paired-end short reads we calculated the relative proportions of cells with two opposite orientations of the invertible promoters of PVR7-12 in different cultures of *B. intestinalis* APC919/174 (**Fig. 3d-e**). We found that the sensitive WT culture is characterised by PVR9 promoter mainly in the ON orientation, while PVR7, PVR8, PVR11 and PVR12 are mainly OFF. In agreement with the RNAseq data, the resistant clone 8T shows a switch of CPS expression from PVR9 towards PVR7, while the WT genotype is largely restored in sensitive revertant sub-clone 8W. Interestingly, other resistant clones showed the PVR9 promoter in mostly the ON orientation, combined with an ON state in one of the three other CPS-associated PVRs. Variable patterns of promoter activation with PVR9 being ON were detectable in the long term *in vitro* and *in vivo* persistence experiments (**Fig. 3d, Fig. S3**).

We suggest, similar to what was observed for a large panel of non-crAss-like phages in *Bacteroides thetaiotaomicron* (Porter et al., 2020), that in the *B. intestinalis*-ΦcrAss001 phage-host pair some of the CPS can be permissive to phage infection, and even serve as phage receptors (possibly PVR9), while some other can be protective (PVR7, PVR8, PVR11 and PVR12) or neutral. We conclude that phase variation of CPS expression leading to phage resistance occurs spontaneously, even in the absence of phage. As a result, a dynamic equilibrium between sensitive and resistant sub-

populations is maintained, which can be shifted towards the resistance phenotype by phage-driven selection. However, a constant switching back to sensitivity provides the phage with a constant supply of sensitive cells, thus assuring its long-term persistence.

Delayed release of ΦcrAss001 progeny leads to multiple echo phage bursts and potentially provides an infection escape mechanism

We previously reported a remarkably low apparent burst size of only 2.5 pfu per cell infected with ΦcrAss001 (Shkoporov et al., 2018). This cannot be explained by failure of phage to infect the majority of cells as only ~2% cells in naïve *B. intestinalis* cultures were phage-resistant due to phase variation. At the same time, >50 particles per cell are visible in TEM images from ultrathin (80 nm) cell sections (**Fig. 2b, d, f**) and at least 20 new copies of phage genome are produced in an infected culture per copy of bacterial genome after 90 min of infection (as shown by metagenomic sequencing above), ruling out the possibility of extremely low progeny counts per infected cell. Further to that, the efficiency of centre of infection tests (EOCI), showed that 56.6±12.7% of cells infected at an MOI=1, and 59.16±27.9% infected at an MOI=10, were capable to give rise to infection centres (plaques) in *B. intestinalis* lawns. Electron microscopic observations of cultures infected at an MOI=1 reveal that >90% of cells show signs of early stages of virion assembly process 40 and 90 minutes after infection (**Fig. S4**). Therefore, the observed low burst size cannot be explained by phase variation-based resistance or low progeny per cell counts and must from an unknown mechanism limiting replication and/or release of phage progeny from a significant fraction of infected cells.

In order to get insights into this mechanism, we performed strand-specific RNAseq analysis of a single phage replication cycle in *B. intestinalis* cells infected at an MOI of 1. Three transcriptional modules can be observed in the ΦcrAss001 genome, which also correlate with ORF orientation and the putative operon organisation of the genome (**Fig. 4a**). The expression of the early genes, located on the right end of the linear phage genome, is initiated between 0 and 10 minutes after phage infection. The predicted products of these genes include a transcriptional regulator, two conserved domain proteins with unknown function and a TROVE domain protein (possible ribonucleoprotein component). A recent study in a distantly related marine crAss-like phage Φ14:2 infecting *Cellulophaga baltica* indicated that a similarly organised operon of early genes is transcribed by a giant virion-associated multi-subunit RNA polymerase [RNAP, (Drobysheva et al., 2020)], ejected into the cell in the course of infection (Holmfeldt et al., 2013). A homologue of this giant polymerase is present in all crAss-like phages and is also encoded by three large ORFs located in the central part of ΦcrAss001 genome (Guerin et al., 2018; Shkoporov et al., 2018; Yutin et al., 2018). Proteomic analysis of the crAss001 virion also indicated the presence of the subunits of the giant polymerase in the assembled phage particle (Shkoporov et al., 2018).

Transcription of the middle and late genes is initiated between 10-30 and 30-60 minutes, respectively, and is likely to depend on the action of the host RNAP [as suggested for Φ14:2 in (Drobysheva et al., 2020)]. The middle genes are largely composed of functions associated with DNA replication and recombination, as well as nucleotide metabolism. Other genes of the same class can be involved in the degradation of host DNA and mRNA (HKD family nuclease, HicA mRNAse). The late genes, occupying the left-hand half of the genome, mainly encode structural proteins of the virion head and tail, as well as proteins participating in the virion assembly (terminase, chaperone) and cell lysis (holin, endolysin). Large ORFs coding for virion-associated

RNAP subunits are located in the approximate centre of the linear genome and are transcribed during middle (gp49, predicted catalytic subunit, and gp50) or late (gp47) transcriptional stages. It is unclear why the temporal separation in RNAP subunit production might be needed. It may be that gp49 and gp50 are involved in transcription of the late genes in the same infection cycle in which they are produced, whereas gp47 is needed solely for the early genes transcription in the next cycle, or plays a role in the packaging, ejection or activation of the RNAP holoenzyme.

Interestingly, there was significant overlap in transcription of early, middle and late genes: once activated, transcripts of each of the three modules persisted through the rest of the replication cycle (**Fig. 4A-b**). The host transcriptional response was largely confined to strong genome-wide inhibition of transcription, occurring between 10-30 minutes preceded by the activation of certain energy metabolism functions at 10 minutes (most notably citrate synthase and iso-citrate dehydrogenase, **Fig. 4b**).

Morphological changes in the infected cells were visible as early as after 45 minutes as the formation of variable-sized electron-light spots (**Fig. 4c**). Ninety minutes into the infection cycle, well after the onset of expression of structural genes, the first intact phage particles (electron-dense spots) begin to appear amongst the electron-light spots. Large clusters of viral particles are visible inside many of the infected cells at 120 minutes. Agreeing with the one step growth curves (**Fig. 4d-e**), cell lysis becomes noticeable at 150 minutes and widespread at 180 minutes. Interestingly, however, a large fraction of cells at 150 minutes remain intact, and only show signs of the early stage of infection with no properly formed phages particles (**Fig. 4f**). This observation can be interpreted as de-synchronisation of the phage replication cycle with some of the cells falling behind the others in terms of infection stage. Supporting this hypothesis is the continued expression of early and middle operon genes, overlapping in timing with late genes. This is further reflected in the one step growth curves, where at an MOI of 1 or 10, a series of discrete, evenly spaced bursts are apparent with a low total progeny output (~3-6 pfu per capita).

Recently, bacteriophages similar to ΦcrAss001 in morphology and genome organisation (**Fig. S5a-b**) were isolated against *B. thetaiotaomicron* (Hryckowian et al., 2020). Phages DAC15 and DAC17 are also capable of long-term persistence in serial broth cultures of *B. thetaiotaomicron* VPI-5482 (**Fig. S5c**) and do not significantly reduce the bacterial population. While the wild-type strain produce eight different phase-variable CPS, a panel of engineered mutants have been developed, which included an acapsular version, as well as eight strains expressing only one of the eight different CPSs, referred to hereafter as CPS1-8 (Porter et al., 2017; Rogers et al., 2013). Phages DAC15 and DAC17 were reported to infect the *cps3*$^{+}$ mutant efficiently, while only showing weak replication in WT VPI-5482 and other single-CPS expressing derivatives, indicating that CPS3 plays a permissive role in phage infection.

In our hands, both DAC phages were able to persist stably in serial daily broth cultures of *cps3*$^{+}$, as well as in WT (albeit at lower levels, **Fig. S5d**). This is despite the fact that an inability to switch to expression of alternative CPSs leads to a very low fraction of pre-existing resistant cells ($< 10^{-5}$) in populations of *cps3*$^{+}$, compared to 52.8±1.2 – 64.2±3.0% of cells resistant to DAC15/ DAC17 in the WT strain. This indicates that the removal of CPS variability leads to greatly reduced resistance to phage but does not eliminate the ability of phage to persist long-term. In one step growth experiments at an MOI=1, DAC15 and DAC17 behaved very similarly to ΦcrAss001, producing a series of bursts and a low apparent output of progeny (**Fig. S5e-f**). However, unlike in *B. intestinalis*-ΦcrAss001 system, infection of *cps3*$^{+}$ mutant at MOI=10 resulted in a single burst of

~160 pfu per capita, a value which is in a much closer agreement with the progeny size observed microscopically (**Fig. S5g**).

This data suggests that a mechanism of gradual release of phage progeny operates in *Bacteroides* cells infected with crAss-like phages ΦcrAss001, DAC15 and DAC17. This mechanism is largely independent of the dynamic phase variation mediated resistance discussed above. It appears that at high MOI the mechanism might become overwhelmed, or that the stress response in cells simultaneously infected by multiple phage particles switches it off. This leads to abrupt cell lysis and release of large phage progeny simultaneously, in a "classical" virulent phage manner.

Discussion

Since their discovery in 2014, crAss-like phages have become one of the most intriguing elements of the human virome. Based largely on metagenomic observations, this group of tailed dsDNA bacteriophages differs significantly from other members of the order Caudovirales in terms of their genome organisation, gene content, virion morphology, life cycle and ecological distribution (Dutilh et al., 2014; Koonin and Yutin, 2020; Shkoporov et al., 2018, 2019). Of special interest is their unexplained, overwhelming prevalence in the gut microbial community, their ability for long term persistence and seemingly benign interaction with their hosts (Shkoporov et al., 2019). The current, provisional classification of crAss-like phages based on gene sharing patterns, lists ten genera (denoted I-X) in four subfamilies (*Alphacrassvirinae*, *Betacrassvirinae*, *Gammacrassvirina*e and *Deltacrassvirinae*). Genus I includes the original p-crAssphage and is by far the most commonly detected and the most abundant member of the family in the human gut, at least in the Western populations (Guerin et al., 2018). However, the only genus that contains a cultured representative is candidate genus VI (*Betacrassvirinae*) which are widespread but only moderately abundant in the human gut. Members of this genus were isolated from human faeces (ΦcrAss001), wastewater effluent (DAC15 and DAC17), and sea water (Φ14:2), infecting *B. intestinalis* (Shkoporov et al., 2018), *B. thetaiotaomicron* (Hryckowian et al., 2020) and *C. baltica*, respectively (Holmfeldt et al., 2013). All these phages were able to lyse target cultures at least partially and produce spots and plaques in a semi-solid agar overlay assay. Phage of genus I and other genera common in the human gut could be grown *in vivo* after transfer into oligoxenic mice or after faecal microbial transplantation of crAssphage-rich microbiota into human patients, and *ex vivo* as part of a native faecal community in a bioreactor, but have not as yet been isolated in pure bacterial cultures (Draper et al., 2018; Dutilh et al., 2014; Reyes et al., 2013; Shkoporov et al., 2019).

We hypothesize that crAss-like phage-host systems encompass a range of behaviours, from one resembling virulent phages that produce plaques but whose replication in pure host cultures and complex microbial communities is typically supported at lower levels; to one similar to temperate phage that produce no plaques but persist in host populations at very high levels. It is notable that, regardless of the degree of virulence of a crAss-like phage, their stable and high-level persistence *in vitro* and *in vivo* has no obvious detrimental effect on the population densities or fitness of their bacterial host. This phenomenon is generally consistent with a temperate mode of replication, but we conclude from our analysis of ΦcrAss001, DAC15 and DAC17 that these viruses are non-lysogenic. Specifically, (i) no cases of related prophages have ever been observed in public databases of bacterial genomes; (ii) no clear lysogeny modules could be identified their genomes; and (iii) lysogens or pseudolysogens could not be obtained experimentally.

Observations of long-term persistence of virulent bacteriophages in the mammalian gut are not unprecedented. Experiments in monoxenic mice revealed that administration of virulent phage fails to lower the levels of target *E. coli* bacteria and often leads to continuous shedding of high phage levels in faeces (Maura et al., 2012; Weiss et al., 2009). Alternative mechanisms of non-lethal, persistent forms of infection were described in virulent phages, including the carrier state and unstable pseudolysogeny in *Campylobacter jejuni*, *Salmonella typhimurium* (phage P22) and *Pseudomonas aeruginosa* (Cenens et al., 2013; Latino et al., 2016; Siringan et al., 2014). In *C. jejuni*, virulent bacteriophages CP8 and CP30A have been shown to maintain equilibrium with their hosts for many generations and to persist intracellularly in an episomal form without integration into the host chromosome. It has also been demonstrated that the carrier state can have a profound effect on bacterial host physiology, such as a major acquisition of self-targeting CRISPR spacers, decreased fitness, loss of colonisation potential and motility in *C. jejuni* (Hooton et al., 2016). More recently a carrier state was described in *P. aeruginosa* infected with ssRNA levivirus LeviOr01 (Pourcel et al., 2017). Infection with LeviOr01 caused dissociation of the sensitive host into two sub-populations: a small subset of phage-carrying superinfection immune cells, spontaneously and continuously releasing phage progeny, and a larger subset of uninfected non-carrier cells. Together, previous observations suggest that unconventional forms of phage infection span a wide taxonomic variety of bacteria and levels of complexity of phages (from *Leviviridae* containing only four genes in their genomes, to *Myoviridae* with hundreds of genes).

The genus *Bacteroides* comprises strictly anaerobic Gram-negative non-sporeforming bacteria, many of which are predominant members of the human gut microbiome and are highly adapted to the gut environment (Wexler and Goodman, 2017). Genome plasticity, extensive regulation of gene expression and high adaptability to changes in their environment are characteristic features of this bacterial group (Comstock and Coyne, 2003). Phase variation of surface structures resulting from DNA inversions catalysed by serine and tyrosine recombinases has been implicated as an important mechanism in *Bacteroides* for adaptation to environmental change, improved fitness, and efficient colonisation of the mammalian gut (Coyne et al., 2003; Jiang et al., 2019; Nakayama-Imaohji et al., 2009, 2016; Porter et al., 2017). Recently, phase variation of multiple surface structures including CPS, S-layer lipoproteins, TonB-dependent nutrient receptors and OmpA-like proteins, has also been implicated in dynamic switching of diverse phage resistance/sensitivity patterns in *B. thetaiotaomicron* (Porter et al., 2020). Furthermore, crAss-like phages DAC15 and DAC17 were shown to preferentially infect a phase variant of *B. thetaiotaomicron* expressing a specific type of CPS (Hryckowian et al., 2020). Recent modelling with phase variable phage receptor in *Haemophilus influenzae* demonstrated the role of phase variation in bacterial “herd immunity”, a phenomenon in phage-host population dynamics where “protective quarantining” of one third of the host cells already confers significant protection against phage attack to the whole population (Turkington et al., 2019).

In this study we shed some light on the mechanisms underpinning persistence of crAss-like phages using the ΦcrAss001-*B. intestinalis* pair as a model. We observed that, similarly to metagenomic findings from the human gut (Shkoporov et al., 2019; Siranosian et al., 2020), a monoxenic mouse model was able to support long term and stable persistence of ΦcrAss001. Bacterial clones recovered from colonised mice showed varied degree of resistance to phage, but no obvious cost with regards to bacterial population density was associated with phage colonisation. We propose that that at least two separate mechanisms operating simultaneously are responsible for observed

persistence *in vitro*: (i) dynamic and reversible acquisition of phage resistance in the host population, dependent on phase variation of CPS; (ii) delayed release or progeny from infected cells, resulting in a pseudolysogenic-like or carrier state phenotype. (**Fig. 5**).

Sustained phage attack resulted in either switching off the PVR9 CPS locus, implicating this structure in phage adsorption, or increased expression of alternative CPS's (PVR7, PVR8, PVR11 and PVR12) with possible protective effects. We propose that the dynamic switching between different CPS types maintains an equilibrium of sensitive and resistant cells, allowing for restricted ("quarantined") phage replication and enabling long term phage persistence and herd immunity in the bacterial population. While phage attack provides an obvious selective force driving switching to resistance states, the force driving a return to sensitivity remains unidentified. In complex microbiota conditions, expression of CPS protective against one phage could make cells sensitive to another phage present in the same environment (Porter et al., 2020), creating an equilibrium of CPS expression states driven by opposing phages. In monoculture, however, such diverse phage selective forces are absent, making the metabolic cost of expression of a particular protective CPS an obvious reason for switching it off. Availability of a single-CPS mutant panel in *B. thetaiotaomicron* prompted us to check whether persistence of DAC15 and DAC17 is still possible despite inability of the strain to evade phage by swapping its CPS types. Indeed, not only persistence in such strain was still possible, but actually occurred at higher levels than in the WT.

We hypothesise that a second mechanism of phage persistence operates in parallel with herd immunity. This is based on the low apparent burst size (despite progeny counts of >50 per cell under the EM), multiple sequential smaller bursts and cells carrying phage progeny without lysing in a timely manner, the high expression of mainly early genes (regulatory proteins) and some of the middle genes (replication functions) in broth cultures of *B. intestinalis* in the presence of phage. Several explanations are possible: (a) carrier state, persistence in the form of fully formed or incompletely formed viral particles in the host cytoplasm; (b) unstable pseudolysogeny, persistence of phage genomes in an episomal form; (c), inhibition of phage reproduction by cellular mechanisms and curing of infected cells. Interestingly, overwhelming the cells with high MOI was enough to overcome this mechanism of gradual release of progeny in *B. thetaiotaomicron* but not in *B. intestinalis*.

We suggest that the interplay between phase variation of phage receptors and the carrier state infection enable highly synchronised replication of a crAss-like phage with its host at a population level, and leads to an equilibrium of phage/host ratio maintained over multiple generations.

It has been proposed that high availability of bacterial prey in aquatic environments and at mucosal surfaces selects for temperate bacteriophage lifestyles and lysogenic mode of replication. Such persistent infection is highly beneficial for the phage and is at least 'affordable' (if not also beneficial) to the host (Knowles et al., 2016; Silveira and Rohwer, 2016). This ecological model has become known as "piggyback-the-winner", as opposed to the "kill-the-winner" model (Silveira and Rohwer, 2016). The mammalian gut presents an example of one of the most densely populated microbial communities, with *Bacteroides* being one of its most abundant and temporally stable bacterial genera (Arumugam et al., 2011; Mehta et al., 2018; Shkoporov et al., 2019). Our expectation was that the majority of bacteriophages in such an environment would be temperate, "piggybacking" on the ecological success of their bacterial hosts (Minot et al., 2013; Norman et al., 2015; Reyes et al., 2010). At the same time our recent metagenomic analysis highlighted the prevalence of apparently virulent bacteriophages in the healthy core virome (Clooney et al., 2019;

Shkoporov et al., 2019). One could hypothesise that crAss-like phages, incapable of classical lysogeny and comprising a large part of these metagenomic sequences, employ alternative life cycle strategies, such as the one highlighted in this this study in order to benefit from "piggyback-the-winner" dynamics.

While the ecological benefits of carrier state infection are obvious for the phage, we can expect that the bacterial host party should also derive certain benefits from this interaction. In addition to exerting a constant selective pressure leading to host diversification through phase variation and point mutations and an improved overall fitness, persistent phage can participate in lateral gene transfer, provide protection from incoming competitor strains and superinfection immunity against cognate phages.

Acknowledgements

This research was conducted with the financial support of Science Foundation Ireland (SFI) under Grant Number SFI/12/RC/2273, a Science Foundation Ireland's Spokes Programme which is co-funded under the European Regional Development Fund under Grant Number SFI/14/SP APC/B3032, and a research grant from Janssen Biotech, Inc. Authors wish to thank Frances O'Brien and Tara O'Driscoll (UCC) for their technical help with germ-free mouse experiment. Authors also wish to thanks Prof. Andrew Hryckowian (University Wisconsin-Madison) for providing phages DAC15, DAC17 and their bacterial hosts.

Author contributions

Conceptualization, A.N.S. and C.H.; Methodology, A.N.S., E.V.K., N.S., C.H. and D.S.; Software, A.N.S.; Formal analysis, A.N.S., E.V.K., D.S. and C.H.; Investigation, A.N.S., E.V.K., C.H. and S.S.; Resources, D.S. and C.H.; Writing – original draft, A.N.S. and E.V.K.; Writing – review and editing, A.N.S., E.V.K., C.H., D.S., R.P.R. and C.H.; Supervision, D.S., C.H. and R.P.R.; Project administration, C.H.; Funding acquisition, C.H. and R.P.R.

Declaration of interests

The authors declare no competing interests.

Figure 1. Long term persistence of crAss-like phages in the gut microbiome and *in vitro*. (a), Persistence of 11 crAss-like phage genomes (belonging to candidate genera I,II,V,VI,VII,X according to Guerin et al. [2018] taxonomy) in faecal VLP fractions of 10 healthy adult individuals over a period of 12-26 months (Shkoporov et al., 2019); **(b)**, Persistence of ΦcrAss001 in the gut of C57BL/6NTac mice (n = 6) mice colonised with ΦcrAss001/*B. intestinalis* APC919/174 mixture at an MOI=1; the control group of mice received oral gavage of *B. intestinalis* only; **(c)**, replication of ΦcrAss001 in exponentially growing culture of *B. intestinalis* (OD600=0.3 at infection with an MOI=1) followed by four daily transfers of phage/host co-culture in fresh broth; bacterial and free phage counts were obtained by plating and plaque assays respectively; **(d)**, VMR determined using shotgun metagenomic sequencing in the same phage/host co-cultures as in (c), with additional samples collected after 18 and 23 daily transfers.

Figure 2. Resistance of *B. intestinalis* APC919/174 to ΦcrAss001 is reversible and associated with capsular polysaccharide alterations and loss of phage adsorption. (a), spotting of $4x10^7$

pfu of ΦcrAss001 on *B. intestinalis* APC919/174 agar overlay results in turbid clearing zone; **(b-f)**, TEM (x9,900-105,000) of ultra-thin sections (80 nm) of samples taken from the centre of the spot shows the presence of un-infected cells amongst lysed cell debris (deb), infected cells with empty virions still attached (Φeh), and cells in the process of division (dic) with phage progeny (Φpro) visible inside of them; **(g) and (h)**, soft agar overlays inoculated with the same number of *B. intestinalis* CFU in the absence and presence of the excess of phage, respectively; **(i)**, phenotypic dissociation of colonies of phage-resistant clone 8, (8W, "white" – phage-sensitive subclone; 8T, "transparent" – phage-resistant subclone); **(j)**, kinetics of ΦcrAss001 adsorption to *B. intestinalis* phage resistant and sensitive clones; vertical axis, concentration of phage in the supernatant; horizontal axis, time passed after addition of phage; R, resistant clones (n=5); Rev, revertant sensitive sub-clones derived from one of the resistant clones; values are mean±SD from three independent experiments; **(k-l)**, ultrathin section TEM visualisation (x60,000) of altered cell surface morphology in phage-resistant clone 8T, compared to phage-sensitive WT strain; lc, loose capsule; cc, compact capsule; cm, cytoplasmic membrane; om, outer membrane.

Figure 3. Structure and transcriptional control of five phase-variable capsular polysaccharide (CPS) operons (PVR7, PVR8, PVR9, PVR11, PVR12) in *B. intestinalis* APC919/174. (a), host transcriptional response in a *B. intestinalis* APC919/174-ΦcrAss001 serial broth co-culture (24-120h *in vitro* persistence) experiment, analysed using RNAseq (values are log2 fold gene transcript expression change relative to the un-infected control from two independent experimental runs); clone-8T, phage resistant derivative of the parental strain; clone-8W, spontaneous phage-sensitive revertant clone; only genes with significantly different expression ($p < 0.001$ in DESeq2, $n = 722$) are shown; genes, associated with phase-variable genomic regions (PVR) are marked with colour bars on top; **(b)**, structure of phase variable operons, encoding five different CPS; protein sequence homologies (tBLASTx) between gene products are shown as coloured parallelograms; two-sided arrows and ON/OFF labels mark positions of invertible promoters; **(c)**, consensus sequence of the regions flanking invertible promoters in CPS biosynthesis loci; approximate transcription start was identified though analysis of RNAseq data; stacked area charts show RNAseq read coverage of regions adjacent to the promoter in four CPS loci; **(d-e)**, fraction or Illumina concordantly-aligned read pairs supporting orientation of invertible promoters in either ON or OFF directions; WT, wild type strain; clones 8T, PhR1-9, phage-resistant derivatives; 8W, phage-sensitive revertant; P18d/P23d, samples in (e) were taken from the long term *in vitro* persistence experiment (also see Fig. S3 for similar data on the long term *in vivo* persistence).

Figure 4. Transcriptional and morphological presentation of ΦcrAss001 infection in a one-step growth experiment. (a), transcription of phage genome 0-120 min after infection revealed using stranded RNAseq; positive and negative strand ORFs and RNAseq coverage levels are shown in blue and red, respectively; plots are representative of two independent experiments; **(b)**, time course of transcriptional responses of host and phage genomes (values are log2 fold gene transcript expression change relative to the previous time point from two independent experimental runs); only genes with significantly different expression of sense DNA strand between any of the successive time points ($p < 0.05$ in DESeq2, $n = 946$) are shown; **(c)**, time-course of morphological changes in *B. intestinalis* cells infected with ΦcrAss001, ultrathin section TEM (x43,000); Φpro, intracellular phage progeny; Φsc, possible "phage scaffolds" in the early stages of virion assembly;

(d-e), enumeration of per capita phage progeny produced in a one-step growth experiment by *B. intestinalis* cells infected with ΦcrAss001 [MOI=1 in panel (d), MOI=10 in panel (e)]; **(f)**, intact cells after first phage burst (150 min), still showing hallmark features of the early and middle infection stages (x6,000).

Figure 5. Model of perpetuated replication of crAss-like phage in *Bacteroides* cultures.

Methods

Resource availability

Lead contact

Further information and requests for data and resources should be directed to and will be fulfilled by Dr. Andrey Shkoporov (andrey.shkoporov@ucc.ie).

Materials availability

Phage ΦcrAss001 and its host *B. intestinalis* APC919/174 are available from DSMZ culture collection under catalogue numbers DSM 109066 and DSM 108646 respectively.

Data and code availability

Raw sequencing data are available from NCBI databases under BioProject PRJNA678472.

Experimental model details

Bacteriophage ΦcrAss001 and related viruses

The host strain *B. intestinalis* APC919/174 was propagated anaerobically on Fastidious Anaerobe Broth (FAB, Neogen, UK) and agar (FAA) at 37°C as described before (Shkoporov et al., 2018). To generate high titer phage lysates, early log phase culture (OD_{600}=0.2; ~$2x10^8$ cfu ml^{-1}) were infected with ΦcrAss001 at an MOI of 1. Cultures were left to grow overnight at 37°C in anaerobic jars, centrifuged for 15 min at 5,200 g and 4°C and filtered through 0.45 µm polyethersulfone (PES) syringe-mounted filter membranes. Plaque and spot assays throughout different experiments were performed after filtering 1 mL of phage/bacteria co-cultures, performing serial dilutions and combining 100 µl of them with 300 µl of a fresh APC919/174 overnight culture in 0.4% bacto agar overlays. Incubations were performed anaerobically at 37°C. Bacteriophages DAC15 and DAC17 (kind gift of Prof. Andrew Hryckowian) and their host strains *Bacteroides thetaiotaomicron* VPI-5482 (WT and *cps3*$^+$) were propagated in the same conditions as *B. intestinalis*/ΦcrAss001.

Germ-free mouse model

The germ-free animal experiment was performed in accordance with the European Communities Council Directive 2010/63/EU under an authorisation issued by the Health Products Regulatory Authority (HPRA, Ireland), with approval from the Animal Experimentation Ethics Committee (AEEC) of University College Cork. Twelve male 13 week old (26-29 g) germ-free C57BL/6N mice (RRID:MGI:5651595, original breeding stock from Taconic, USA; bred in house) were housed in groups of 2-3 mice in HEPA filtered individually ventilated cages to maintain germ-free status. All dosing and faecal sampling occurred under sterile conditions in a biosafety cabinet to ensure there was no confounding colonisation. Group 1 (n = 6) were orally dosed on three

successive days with 100 µl of phage/bacteria suspension (10^9 cfu of bacteria, $2x10^8$ pfu of phage per gavage). Group 2 were orally dosed with bacteria only (10^9 cfu per gavage). Faecal samples were collected for 146 days after the first dose (days 3, 6-10, 14, 17, 24, 31, 38, 45, 59, 87, 93, 101, 108, 115, 121, 129, 136, 146) and subjected to plating and plaque assays for enumeration of bacteria and phage (**Fig. 1b**). On the last day of the experiment animals were humanely euthanised by cervical dislocation.

Method details

In vitro experiments with crAss-like phages

Phage adsorption experiments (**Fig. 2j**) was conducted in aerobic conditions at room temperature on cells from an overnight *Bacteroides* culture (10 mL, optical density adjusted to OD_{600}=0.2), triple washed with growth medium and resuspended in the same media volume before the experiment. Phage was applied at an MOI=1, aliquots were removed, filtered as described above and subjected to plaque assays 5 and 20 min after addition of phage.

Efficiency of bacterial plating (EOP) in the presence of phage (**Fig. 2g-h**) was conducted as follows: Serial tenfold dilutions of overnight *Bacteroides* cultures were inoculated into 3 mL of semi-solid FAA (0.4% agar) with or without addition of 100 µL high-titre phage (~10^{10} pfu mL^{-1}) and poured onto 100 mm diameter FAA agar plates. Efficiency of lysogeny was determined as a percentage of colonies observed on phage-containing overlays relative to the total counts on negative control overlays after 48 hours of anaerobic incubation at 37°C.

In vitro phage persistence experiment (**Figs. 1c-d, 3a, 3d, S5d**) was performed as follows: ten millilitre liquid cultures (n=3) of *Bacteroides* were infected at OD_{600}=0.2 and MOI=1, and incubated overnight. The co-culture was then transferred daily, for five days in fresh FAB medium at 1:50 ratio.

One-step growth curves (**Fig. 4d-e, S5e-g**) were built as follows: early logarithmic phase (OD_{600}=0.2) cultures of *Bacteroides* (20 mL) were infected at an MOI of 1 or 10 for 5 min at room temperature, followed by centrifugation at 5,200 g, 4°C for 15 min, removal of supernatant and re-suspending of the infected cells in fresh FAB medium. Incubation was continued anaerobically at 37°C for further 225 min with removal of 1 mL samples every 15 min. Samples were filtered through 0.45 µm pore PES filters and subjected to standard plaque assays with appropriate dilutions. Efficiency of centre of infection (EOCI) was determined by doing plaque assays with infected cells at the same time intervals but without filtration step.

Transmission electron miscroscopy

Ultrathin section TEM of *Bacteroides* cells grown in broth cultures (**Fig. 2k-l**) or embedded in semi-solid agar (**Figs. 2b-f, 4c, 4f, S4**) were performed as follows. Pellets from 1 mL broth cultures or agar overlay fragments (~100µL volume) were immediately fixed and stored in 1 mL of 2% (v/v) glutaraldehyde, 1.5% (w/v) parafolmaldehyde, 75 mM Tris-HCl pH 7.5 solution. Samples were post fixed with 1% Osmium tetroxide in 0.1 M Sorenson's phosphate buffer for 1 hour at room temperature. A series of graded dehydrations were performed with increasing ethanol concentrations (30%, 50%, 70%, 100%; cells from broth cultures were pelleted by centrifugation between steps). Dehydrated samples were embedded in Epon resin. Briefly, dehydrated samples were transferred into 100% acetone and then 50:50 acetone:Epon resin for a minimum of 1 hour. Samples were then put in 100% Epon resin at 37°C for 2 hours. Resin was polymerised at 60°C for a minimum of 24

hours. Embedded samples were sectioned at 80 nm thickness onto copper grids using a Leica UC6 ultramicrotome. Samples were stained with 2% uranyl acetate for 20 minutes and 3 % lead citrate for 5 minutes. Grids were then imaged on a FEI Tecnai 120 at 120 kV accelerating voltage.
TEM of purified phage particles (**Figs. S5a-b**) was performed as described before (Shkoporov et al., 2018).

Shotgun sequencing and analysis of bacterial genomes

Shotgun sequencing on Illumina platform was performed for parental strain APC919/174 (**Figs. 3b, 3e, S1, S2**), resistant clones PhR1-9, 8T and spontaneous sensitive revertant derivative (8W) of the latter (**Figs. 3e, S1, S2**), as well as samples from *in vitro* phage persistence experiment and faecal samples from mice colonized with ΦcrAss001/*B. intestinalis* phage-host pair (**Figs. 3d, S3**). BioSample accession number are SAMN16802447-SAMN16802559 and SAMN16803214.
Genomic DNA was extracted from bacterial cultures and phage-host co-cultures using DNeasy Blood & Tissue Kit (Qiagen) in accordance with the manufacturer's Gram-negative bacteria protocol. Faecal DNA was extracted using QIAamp Fast DNA Stool Mini Kit (Qiagen). Concentration of DNA was determined using the Qubit dsDNA HS kit and the Qubit 3 fluorometer (Invitrogen/ThermoFisher Scientific). One hundred nanograms of purified DNA sample were sheared with M220 Focused-Ultrasonicator (Covaris) applying the 350 bp DNA fragment length settings (peak power 50 W, duty factor 20 %, 200 cycles per burst, total duration of 65 s). Random shotgun libraries were prepared from genomic DNA using TruSeq Nano Library Preparation Kit (Illumina, cat #20015964) with dual-indexing following the standard manufacturer’s protocol. Paired-end sequencing with 2×150 nt chemistry was performed on HiSeq 4000 platform at Eurofins Genomics.
The quality of raw sequences (SRA database records SRR13062103-SRR13062215) was assessed using FastQC v0.11.5. TruSeq adapters were removed with cutadapt v2.4. To trim sequences and remove low quality reads, Trimmomatic v0.36 was applied using the following parameters: ‘SLIDINGWINDOW:4:20 MINLEN:60 HEADCROP:10’, yielding 2.2-9.7 million reads per sample (median 5.9 million).
For long read Oxford Nanopore sequencing genomic DNA from APC919/174, 8T, 8W, Phr5 and Phr5-1 (sensitive derivative of the resistant clone Phr5) was extracted as follows. Cells from two mL of overnight cultures were collected by centrifugation at 5,000 g for 10 min, washed by resuspending in 1 mL of TES (50 mM NaCl, 100 mM Tris-HCl, 70 mM disodium EDTA, pH 8.0) and re-centrifuged. After resuspending cell pellets in 0.4 mL of TES supplemented with 25% w/v sucrose and 30 mg mL^{-1} of lysozyme, 50 U of RNase I (Fisher Scientific) were added and samples were incubated at 42°C for 1 hour. Cells were then lysed by addition of 20 µL of 10% (w/v) sarkosyl and 5 µL of 20 mg mL^{-1} proteinase K solutions with incubation at 37°C until complete clearing of the lysate (30-60 min). The obtained lysates were diluted by adding 350 µL of TES and 16 µL of 5M NaCl and gently extracted twice with equal volume of 25:24:1 phenol:chloroform:isoamyl alcohol mix with room temperature centrifugation at 8,000 g for 5 min. This was followed by a similarly done extraction by an equal volume of chloroform. Finally, aqueous phase was gently mixed with 2 volumes of 96% ethanol and DNA was pelleted by centrifugation at 8,000 g, 4°C for 15 min. Pellets were rinsed with 1 mL of 70% ethanol, air dried and resuspended in 50 µL TE (10 mM Tris-HCl, 0.1 mM disodium EDTA, pH 8.0) by overnight incubation at 4°C.

Long-read sequencing libraries (SRR13062400, SRR13062401, SRR13062402, SRR13062326, SRR13062327) were prepared using Oxford Nanopore Rapid Barcoding Kit (SQK-RBK004) and pooled. The pooled library was then loaded onto R9 version flowcell (FLO-MIN106D) and sequenced in a MinION sequencer (Oxford Nanopore) for 48 hours. Sequencing data was then basecalled, quality-filtered and de-multiplexed using Guppy v3.1.5. This yielded a total of 299,317 reads of 1,882±4,697 nt length (median±IQR) for APC919/174, 27,348 reads of 11,268±24,836 nt length for 8T, 57,259 reads of 10,529±21,955 nt length for 8W, 31,238 reads of 13,673±32,494 nt length for Phr5, and 6,547 reads of 4,207±16,442 nt length for Phr5.

Trimmed and filtered Illumina reads and raw Oxford Nanopore reads were used for hybrid assemblies of the genomes of strains APC919/174, 8T and 8W using SPAdes assembler v3.13.0 in 'careful' mode. This resulted in complete circular contigs of 5,785,761 bp, 5,785,768 bp and 5,785,766 bp respectively. Genomes were annotated using RASTtk and PGAP pipelines and deposited in NCBI Genbank under accessions numbers CP041379, CP064941 and CP064940. Completed genomes were aligned using progressive MAUVE algorithm (version 2015-02-13) to identify regions of major recombination (**Fig. S1**).

For detection of PVR promoter inversions and variant analysis in the *in vitro* co-culture and mouse colonisation experiments (**Figs. 3d-e, S3b**) paired Illumina reads were mapped to the assembled APC919/174 as a reference. Reads were aligned using bowtie2 v2.3.4.1 in the end-to-end mode. Alignments were sorted, indexed and converted into counts tables using samtools v1.7.

For detection of genomic recombination on a single read level, sufficiently long Oxford Nanopore reads (> 1000 nt) were aligned against APC919/174 reference genome using BLASTn v2.10.0 with e-value cut-off of 1e-20. Individual alignments were retained only if length was >200 nt with identity of >90%. Next, reads were identified containing internally inverted alignments or blocks of aligned sequence corresponding to coordinates in the reference genome shifted >200 nt relative to other aligned blocks inside the same read. Such blocks of inconsistently aligned sequence were deemed as evidence of recombination events dynamically unfolding inside an individual clonal culture. Starting coordinates of these misaligned blocks were then plotted against the APC919/174 reference genome in a histogram with 1000 nt long bins and hotsposts of recombination were identified (**Fig. S2**).

RNAseq procedures

Transcriptomic analysis of ΦcrAss001/*B. intestinalis* co-cultures was conducted for *in vitro* phage persistence experiment (**Fig. 3a, 3c**; BioSamples SAMN16809412-SAMN16809423) and one-step growth experiment (**Fig. 4a-b**; BioSamples SAMN16810643-SAMN16810654).

One millilitre culture aliquots were pelleted by centrifugation for 3 min at 17,000 g. Pellets were immediately lysed using 1 mL of TRIzol reagent (ThermoFisher Scientific). Total bacterial RNA was extracted using the standard manufacturers protocol. Extracted RNA (20 µL) was treated with 2U TURBO DNase (ThermoFisher Scientific), further purified using RNeasy Mini Kit (Qiagen) and assayed for RNA integrity and quantity on Agilent Bioanalyzer using 6000 RNA Nano Kit. Stranded RNA-seq libraries were prepared from 1 µg total RNA using ScriptSeq v2 Complete kit for bacteria (Epicentre) and sequenced on Illumina NovaSeq 6000 platform at GENEWIZ. Read quality checks, filtration and trimming was performed as described above in *Shotgun sequencing and analysis of bacterial genomes*.

Reads were then mapped to ΦcrAss001 and *B. intestinalis* APC919/174 reference genomes (NCBI accession numbers MH675552 and CP041379 respectively) using bowtie2 v2.3.4.1 in the end-to-end mode. Alignments were sorted by DNA strand and indexed using samtools v1.7. Samtools 'mpileup' command was used to calculate read coverage per nucleotide position in both genomes. Read coverage tables were then imported into R environment using data.table library v1.12.8. Mean coverage values were calculated per feature (protein-coding genes, structural and non-coding RNAs) for both sense and antisense strand and compared between time points using DESeq2 with Wald test and parametric fit.

Quantification and statistical analysis

Bacterial colonisation levels *in vivo* in the presence or absence of phage (**Fig. 1b**) were compared using Kruskal-Wallis test with FDR correction and were all found to be insignificantly different, except for days 31 and 38 ($p < 0.05$). Adsorption of crAss001 to sensitive and resistant bacterial variants (**Fig. 1b**) was compared using Kruskal-Wallis test with Bonferroni correction and was found significantly different ($p < 0.05$). Analysis of differentially abundant transcripts (**Figs. 3a, 4b**) was performed using DESeq2. Only genes showing significant change ($p < 0.001$ for host genes in in vitro persistence experiment, **Fig. 3a**, and $p < 0.05$ for both phage and host genes in one step growth experiment, **Fig. 4b**) between any of the consecutive time points are displayed. Bacterial genes differentially affected by mutations between the two groups of animals (phage and no phage, **Fig. S3b**) in mouse colonisation experiment were selected using exact Fisher's test ($p < 0.05$ with FDR correction).

References

Arumugam, M., Raes, J., Pelletier, E., Le Paslier, D., Yamada, T., Mende, D.R., Fernandes, G.R., Tap, J., Bruls, T., Batto, J.-M., et al. (2011). Enterotypes of the human gut microbiome. Nature *473*, 174–180.

Bolam, D.N., and van den Berg, B. (2018). TonB-dependent transport by the gut microbiota: novel aspects of an old problem. Current Opinion in Structural Biology *51*, 35–43.

Cenens, W., Mebrhatu, M.T., Makumi, A., Ceyssens, P.-J., Lavigne, R., Houdt, R.V., Taddei, F., and Aertsen, A. (2013). Expression of a Novel P22 ORFan Gene Reveals the Phage Carrier State in Salmonella Typhimurium. PLOS Genetics *9*, e1003269.

Clooney, A.G., Sutton, T.D.S., Shkoporov, A.N., Holohan, R.K., Daly, K.M., O'Regan, O., Ryan, F.J., Draper, L.A., Plevy, S.E., Ross, R.P., et al. (2019). Whole-Virome Analysis Sheds Light on Viral Dark Matter in Inflammatory Bowel Disease. Cell Host & Microbe *26*, 764-778.e5.

Comstock, L.E., and Coyne, M.J. (2003). Bacteroides thetaiotaomicron: a dynamic, niche-adapted human symbiont. BioEssays *25*, 926–929.

Coyne, M.J., Weinacht, K.G., Krinos, C.M., and Comstock, L.E. (2003). Mpi recombinase globally modulates the surface architecture of a human commensal bacterium. PNAS *100*, 10446–10451.

Draper, L.A., Ryan, F.J., Smith, M.K., Jalanka, J., Mattila, E., Arkkila, P.A., Ross, R.P., Satokari, R., and Hill, C. (2018). Long-term colonisation with donor bacteriophages following successful faecal microbial transplantation. Microbiome *6*, 220.

Drobysheva, A.V., Panafidina, S.A., Kolesnik, M.V., Klimuk, E.I., Minakhin, L., Yakunina, M.V., Borukhov, S., Nilsson, E., Holmfeldt, K., Yutin, N., et al. (2020). Structure and function of virion RNA polymerase of a crAss-like phage. Nature 1–4.

Dutilh, B.E., Cassman, N., McNair, K., Sanchez, S.E., Silva, G.G.Z., Boling, L., Barr, J.J., Speth, D.R., Seguritan, V., Aziz, R.K., et al. (2014). A highly abundant bacteriophage discovered in the unknown sequences of human faecal metagenomes. Nature Communications *5*, 4498.

Edwards, R.A., Vega, A.A., Norman, H.M., Ohaeri, M., Levi, K., Dinsdale, E.A., Cinek, O., Aziz, R.K., McNair, K., Barr, J.J., et al. (2019). Global phylogeography and ancient evolution of the widespread human gut virus crAssphage. Nature Microbiology *4*, 1727–1736.

Foley, M.H., Cockburn, D.W., and Koropatkin, N.M. (2016). The Sus operon: a model system for starch uptake by the human gut Bacteroidetes. Cell. Mol. Life Sci. *73*, 2603–2617.

Guerin, E., Shkoporov, A., Stockdale, S.R., Clooney, A.G., Ryan, F.J., Sutton, T.D.S., Draper, L.A., Gonzalez-Tortuero, E., Ross, R.P., and Hill, C. (2018). Biology and Taxonomy of crAss-like Bacteriophages, the Most Abundant Virus in the Human Gut. Cell Host & Microbe *24*, 653-664.e6.

Holmfeldt, K., Solonenko, N., Shah, M., Corrier, K., Riemann, L., VerBerkmoes, N.C., and Sullivan, M.B. (2013). Twelve previously unknown phage genera are ubiquitous in global oceans. PNAS *110*, 12798–12803.

Honap, T.P., Sankaranarayanan, K., Schnorr, S.L., Ozga, A.T., Warinner, C., and Jr, C.M.L. (2020). Biogeographic study of human gut-associated crAssphage suggests impacts from industrialization and recent expansion. PLOS ONE *15*, e0226930.

Hooton, S.P.T., Brathwaite, K.J., and Connerton, I.F. (2016). The Bacteriophage Carrier State of Campylobacter jejuni Features Changes in Host Non-coding RNAs and the Acquisition of New Host-derived CRISPR Spacer Sequences. Front. Microbiol. *7*.

Hryckowian, A.J., Merrill, B.D., Porter, N.T., Van Treuren, W., Nelson, E.J., Garlena, R.A., Russell, D.A., Martens, E.C., and Sonnenburg, J.L. (2020). Bacteroides thetaiotaomicron-Infecting Bacteriophage Isolates Inform Sequence-Based Host Range Predictions. Cell Host & Microbe *28*, 371-379.e5.

Jiang, X., Hall, A.B., Arthur, T.D., Plichta, D.R., Covington, C.T., Poyet, M., Crothers, J., Moses, P.L., Tolonen, A.C., Vlamakis, H., et al. (2019). Invertible promoters mediate bacterial phase variation, antibiotic resistance, and host adaptation in the gut. Science *363*, 181–187.

Knowles, B., Silveira, C.B., Bailey, B.A., Barott, K., Cantu, V.A., Cobián-Güemes, A.G., Coutinho, F.H., Dinsdale, E.A., Felts, B., Furby, K.A., et al. (2016). Lytic to temperate switching of viral communities. Nature *531*, 466–470.

Koonin, E.V., and Yutin, N. (2020). The crAss-like Phage Group: How Metagenomics Reshaped the Human Virome. Trends in Microbiology *28*, 349–359.

Latino, L., Midoux, C., Hauck, Y., Vergnaud, G., and Pourcel, C. (2016). Pseudolysogeny and sequential mutations build multiresistance to virulent bacteriophages in Pseudomonas aeruginosa. Microbiology *162*, 748–763.

Lourenço, M., De Sordi, L., and Debarbieux, L. (2018). The Diversity of Bacterial Lifestyles Hampers Bacteriophage Tenacity. Viruses *10*, 327.

Lourenço, M., Chaffringeon, L., Lamy-Besnier, Q., Pédron, T., Campagne, P., Eberl, C., Bérard, M., Stecher, B., Debarbieux, L., and Sordi, L.D. (2020). The Spatial Heterogeneity of the Gut Limits Predation and Fosters Coexistence of Bacteria and Bacteriophages. Cell Host & Microbe *28*, 390-401.e5.

Maura, D., Morello, E., Merle, L. du, Bomme, P., Bouguénec, C.L., and Debarbieux, L. (2012). Intestinal colonization by enteroaggregative Escherichia coli supports long-term bacteriophage replication in mice. Environmental Microbiology *14*, 1844–1854.

Mehta, R.S., Abu-Ali, G.S., Drew, D.A., Lloyd-Price, J., Subramanian, A., Lochhead, P., Joshi, A.D., Ivey, K.L., Khalili, H., Brown, G.T., et al. (2018). Stability of the human faecal microbiome in a cohort of adult men. Nature Microbiology *3*, 347–355.

Minot, S., Bryson, A., Chehoud, C., Wu, G.D., Lewis, J.D., and Bushman, F.D. (2013). Rapid evolution of the human gut virome. Proc Natl Acad Sci U S A *110*, 12450–12455.

Nakayama-Imaohji, H., Hirakawa, H., Ichimura, M., Wakimoto, S., Kuhara, S., Hayashi, T., and Kuwahara, T. (2009). Identification of the Site-Specific DNA Invertase Responsible for the Phase Variation of SusC/SusD Family Outer Membrane Proteins in Bacteroides fragilis. Journal of Bacteriology *191*, 6003–6011.

Nakayama-Imaohji, H., Hirota, K., Yamasaki, H., Yoneda, S., Nariya, H., Suzuki, M., Secher, T., Miyake, Y., Oswald, E., Hayashi, T., et al. (2016). DNA Inversion Regulates Outer Membrane Vesicle Production in Bacteroides fragilis. PLOS ONE *11*, e0148887.

Norman, J.M., Handley, S.A., Baldridge, M.T., Droit, L., Liu, C.Y., Keller, B.C., Kambal, A., Monaco, C.L., Zhao, G., Fleshner, P., et al. (2015). Disease-specific Alterations in the Enteric Virome in Inflammatory Bowel Disease. Cell *160*, 447–460.

Oude Munnink, B.B., Canuti, M., Deijs, M., de Vries, M., Jebbink, M.F., Rebers, S., Molenkamp, R., van Hemert, F.J., Chung, K., Cotten, M., et al. (2014). Unexplained diarrhoea in HIV-1 infected individuals. BMC Infectious Diseases *14*, 22.

Porter, N.T., Canales, P., Peterson, D.A., and Martens, E.C. (2017). A Subset of Polysaccharide Capsules in the Human Symbiont Bacteroides thetaiotaomicron Promote Increased Competitive Fitness in the Mouse Gut. Cell Host & Microbe *22*, 494-506.e8.

Porter, N.T., Hryckowian, A.J., Merrill, B.D., Fuentes, J.J., Gardner, J.O., Glowacki, R.W.P., Singh, S., Crawford, R.D., Snitkin, E.S., Sonnenburg, J.L., et al. (2020). Phase-variable capsular polysaccharides and lipoproteins modify bacteriophage susceptibility in Bacteroides thetaiotaomicron. Nature Microbiology *5*, 1170–1181.

Pourcel, C., Midoux, C., Vergnaud, G., and Latino, L. (2017). A carrier state is established in Pseudomonas aeruginosa by phage LeviOr01, a newly isolated ssRNA levivirus. Journal of General Virology, *98*, 2181–2189.

Reyes, A., Haynes, M., Hanson, N., Angly, F.E., Heath, A.C., Rohwer, F., and Gordon, J.I. (2010). Viruses in the fecal microbiota of monozygotic twins and their mothers. Nature *466*, 334–338.

Reyes, A., Wu, M., McNulty, N.P., Rohwer, F.L., and Gordon, J.I. (2013). Gnotobiotic mouse model of phage–bacterial host dynamics in the human gut. Proc Natl Acad Sci U S A *110*, 20236–20241.

Rogers, T.E., Pudlo, N.A., Koropatkin, N.M., Bell, J.S.K., Balasch, M.M., Jasker, K., and Martens, E.C. (2013). Dynamic responses of Bacteroides thetaiotaomicron during growth on glycan mixtures. Molecular Microbiology *88*, 876–890.

Scanlan, P.D. (2017). Bacteria–Bacteriophage Coevolution in the Human Gut: Implications for Microbial Diversity and Functionality. Trends in Microbiology *25*, 614–623.

Shkoporov, A.N., Khokhlova, E.V., Fitzgerald, C.B., Stockdale, S.R., Draper, L.A., Ross, R.P., and Hill, C. (2018). ΦCrAss001 represents the most abundant bacteriophage family in the human gut and infects Bacteroides intestinalis. Nature Communications *9*, 4781.

Shkoporov, A.N., Clooney, A.G., Sutton, T.D.S., Ryan, F.J., Daly, K.M., Nolan, J.A., McDonnell, S.A., Khokhlova, E.V., Draper, L.A., Forde, A., et al. (2019). The Human Gut Virome Is Highly Diverse, Stable, and Individual Specific. Cell Host & Microbe *26*, 527-541.e5.

Silveira, C.B., and Rohwer, F.L. (2016). Piggyback-the-Winner in host-associated microbial communities. Npj Biofilms and Microbiomes *2*, 16010.

Siranosian, B.A., Tamburini, F.B., Sherlock, G., and Bhatt, A.S. (2020). Acquisition, transmission and strain diversity of human gut-colonizing crAss-like phages. Nature Communications *11*, 280.

Siringan, P., Connerton, P.L., Cummings, N.J., and Connerton, I.F. (2014). Alternative bacteriophage life cycles: the carrier state of Campylobacter jejuni. Open Biology *4*, 130200.

Turkington, C.J.R., Morozov, A., Clokie, M.R.J., and Bayliss, C.D. (2019). Phage-Resistant Phase-Variant Sub-populations Mediate Herd Immunity Against Bacteriophage Invasion of Bacterial Meta-Populations. Front. Microbiol. *10*.

Weiss, M., Denou, E., Bruttin, A., Serra-Moreno, R., Dillmann, M.-L., and Brüssow, H. (2009). In vivo replication of T4 and T7 bacteriophages in germ-free mice colonized with Escherichia coli. Virology *393*, 16–23.

Wexler, A.G., and Goodman, A.L. (2017). An insider's perspective: Bacteroides as a window into the microbiome. Nature Microbiology *2*, 1–11.

Yutin, N., Makarova, K.S., Gussow, A.B., Krupovic, M., Segall, A., Edwards, R.A., and Koonin, E.V. (2018). Discovery of an expansive bacteriophage family that includes the most abundant viruses from the human gut. Nature Microbiology *3*, 38–46.

Yutin, N., Benler, S., Shmakov, S.A., Wolf, Y.I., Tolstoy, I., Rayko, M., Antipov, D., Pevzner, P.A., and Koonin, E.V. (2020). Unique genomic features of crAss-like phages, the dominant component of the human gut virome. BioRxiv 2020.07.20.212944.

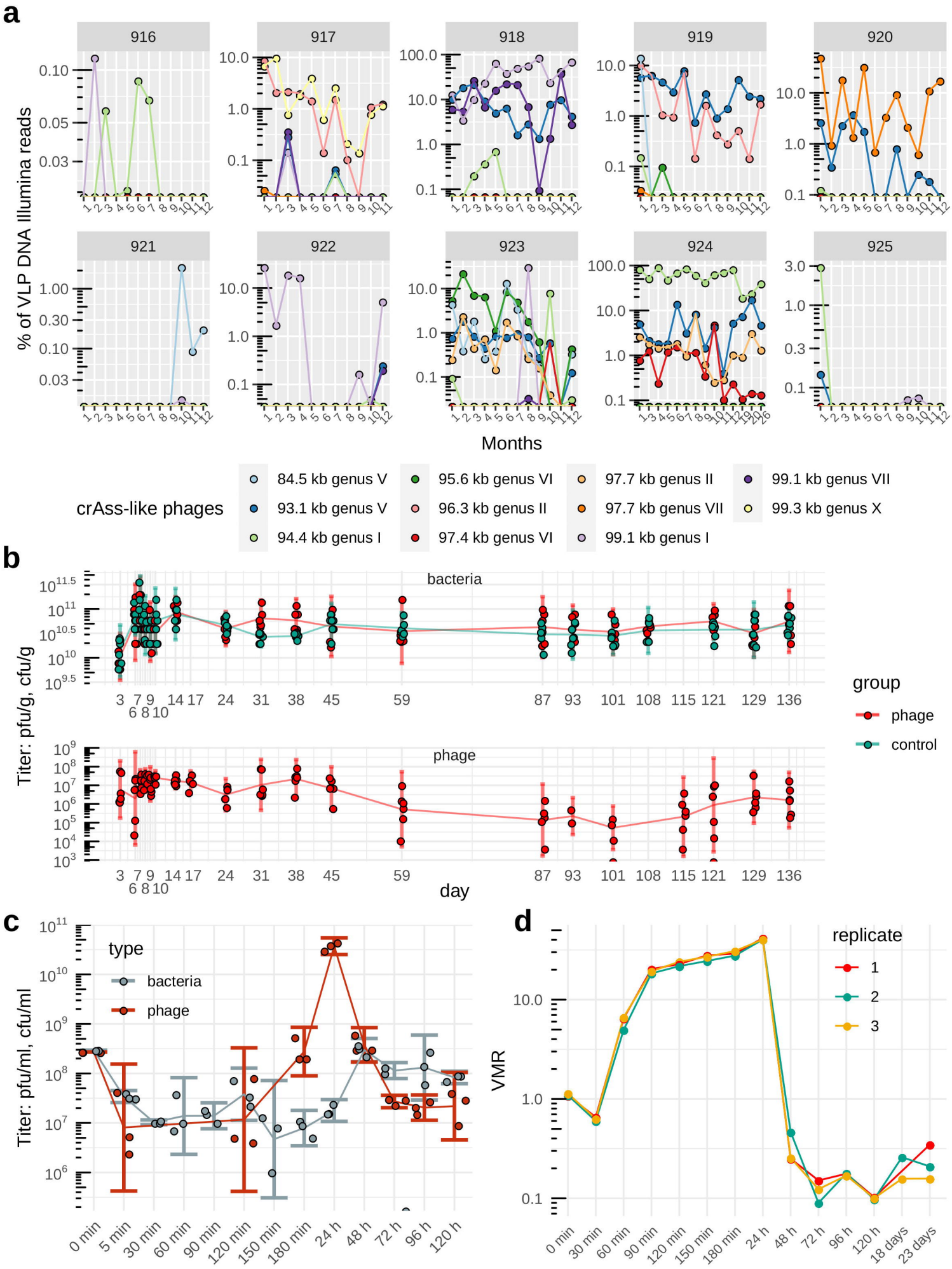
a
916
917
918
919
920
921
922
923
924
925
% of VLP DNA Illumina reads
Months
crAss-like phages
84.5 kb genus V
93.1 kb genus V
94.4 kb genus I
95.6 kb genus VI
96.3 kb genus II
97.4 kb genus VI
97.7 kb genus II
97.7 kb genus VII
99.1 kb genus I
99.1 kb genus VII
99.3 kb genus X
b
bacteria
phage
Titer: pfu/g, cfu/g
day
group
phage
control
c
type
bacteria
phage
Titer: pfu/ml, cfu/ml
0 min
5 min
30 min
60 min
90 min
120 min
150 min
180 min
24 h
48 h
72 h
96 h
120 h
d
replicate
1
2
3
VMR
0 min
30 min
60 min
90 min
120 min
150 min
180 min
24 h
48 h
72 h
96 h
120 h
18 days
23 days

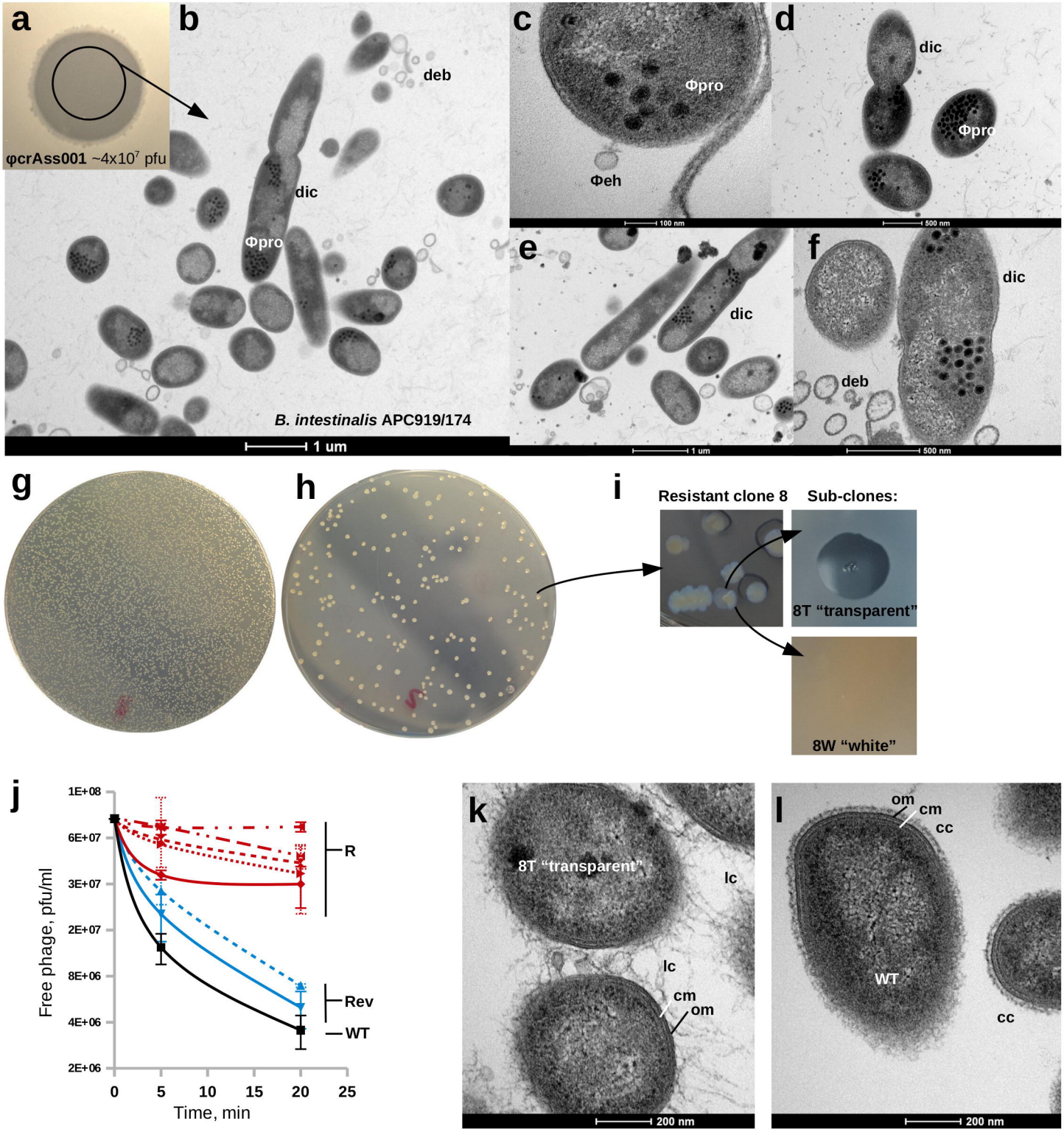
a
φcrAss001 ~4x10^7 pfu
b
deb
dic
Φpro
B. intestinalis APC919/174
1 um
c
Φpro
Φeh
100 nm
d
dic
Φpro
500 nm
e
dic
1 um
f
dic
deb
500 nm
g
h
i
Resistant clone 8
Sub-clones:
8T "transparent"
8W "white"
j
Free phage, pfu/ml
1E+08
6E+07
3E+07
2E+07
8E+06
4E+06
2E+06
0
5
10
15
20
25
Time, min
R
Rev
WT
k
8T "transparent"
lc
lc
cm
om
200 nm
l
om
cm
cc
WT
cc
200 nm

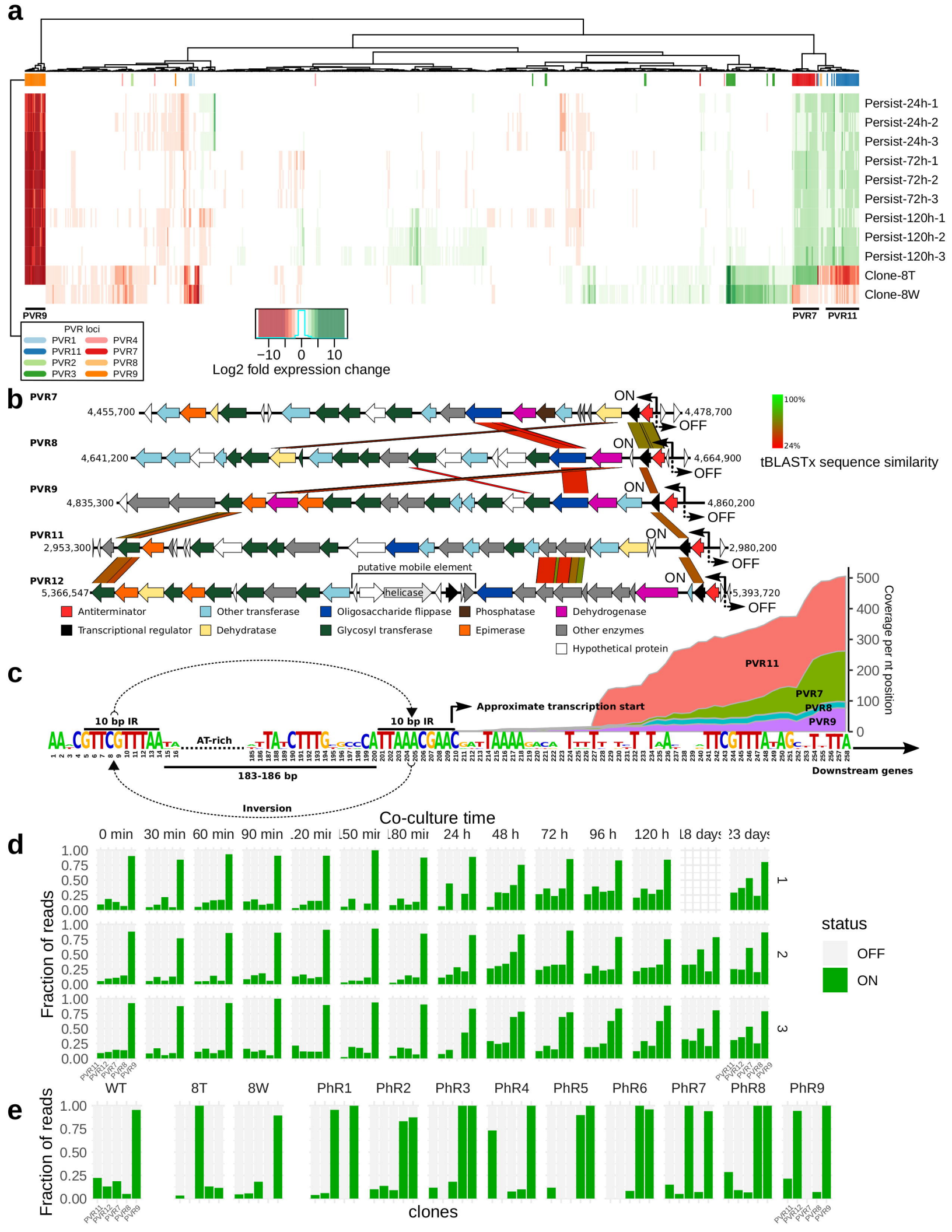
a
Persist-24h-1
Persist-24h-2
Persist-24h-3
Persist-72h-1
Persist-72h-2
Persist-72h-3
Persist-120h-1
Persist-120h-2
Persist-120h-3
Clone-8T
Clone-8W
PVR9
PVR7
PVR11
PVR loci
PVR1
PVR11
PVR2
PVR3
PVR4
PVR7
PVR8
PVR9
−10
0
10
Log2 fold expression change
b
PVR7
4,455,700
ON
4,478,700
OFF
PVR8
4,641,200
ON
4,664,900
OFF
PVR9
4,835,300
ON
4,860,200
OFF
PVR11
2,953,300
ON
2,980,200
OFF
PVR12
5,366,547
putative mobile element
helicase
ON
5,393,720
OFF
100%
24%
tBLASTx sequence similarity
Antiterminator
Other transferase
Oligosaccharide flippase
Phosphatase
Dehydrogenase
Transcriptional regulator
Dehydratase
Glycosyl transferase
Epimerase
Other enzymes
Hypothetical protein
c
10 bp IR
AT-rich
10 bp IR
183-186 bp
Inversion
Approximate transcription start
PVR11
PVR7
PVR8
PVR9
Coverage per nt position
Downstream genes
d
Co-culture time
0 min
30 min
60 min
90 min
24 h
48 h
72 h
96 h
120 h
Fraction of reads
status
OFF
ON
e
WT
8T
8W
PhR1
PhR2
PhR3
PhR4
PhR5
PhR6
PhR7
PhR8
PhR9
Fraction of reads
clones

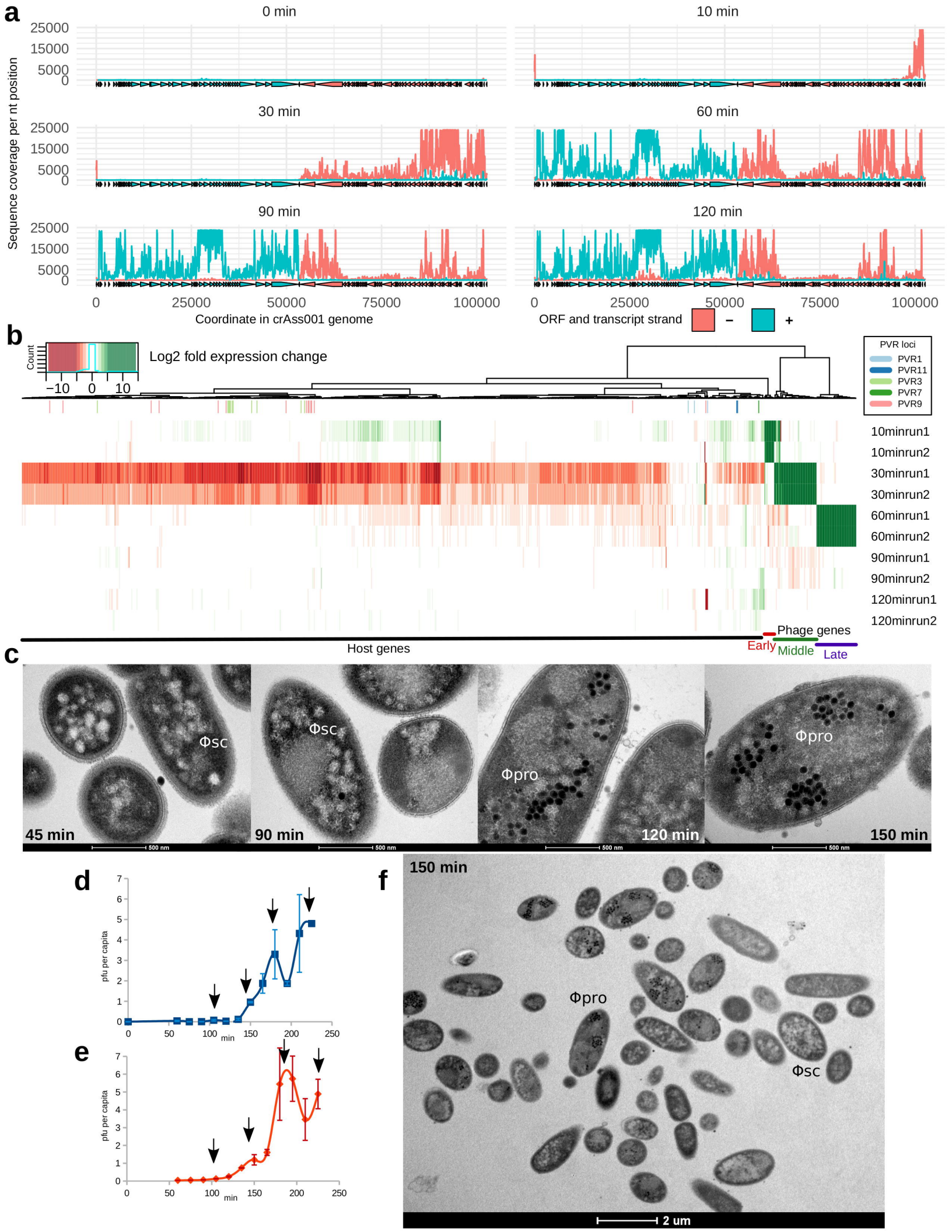
a
0 min
10 min
30 min
60 min
90 min
120 min
Sequence coverage per nt position
25000
15000
5000
0
0
25000
50000
75000
100000
Coordinate in crAss001 genome
ORF and transcript strand
−
+
b
Count
Log2 fold expression change
−10
0
10
PVR loci
PVR1
PVR11
PVR3
PVR7
PVR9
10minrun1
10minrun2
30minrun1
30minrun2
60minrun1
60minrun2
90minrun1
90minrun2
120minrun1
120minrun2
Host genes
Phage genes
Early
Middle
Late
c
Φsc
Φsc
Φpro
Φpro
45 min
90 min
120 min
150 min
500 nm
d
pfu per capita
min
e
pfu per capita
min
f
150 min
Φpro
Φsc
2 um

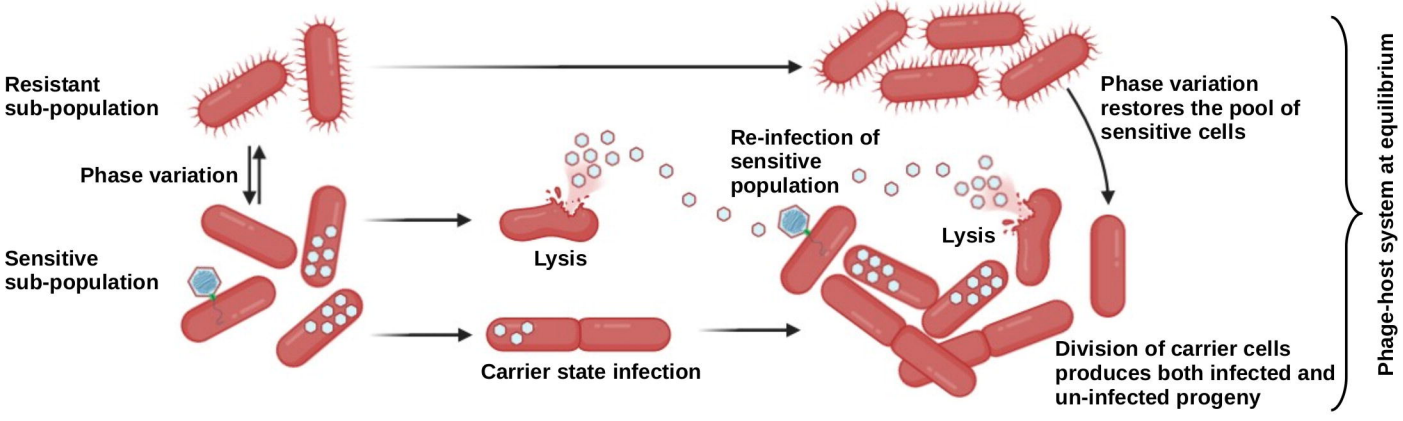
Resistant sub-population
Phase variation
Sensitive sub-population
Lysis
Carrier state infection
Re-infection of sensitive population
Lysis
Phase variation restores the pool of sensitive cells
Division of carrier cells produces both infected and un-infected progeny
Phage-host system at equilibrium